

Evaluating the performance of soil nailing in slope stability under complex conditions

Prashant Ramteke* & Anil Kumar Sahu

Department of Civil Engineering, Delhi Technological University, Delhi 110 042, India

Received: 25 June 2025; accepted: 14 September 2025

Soil nailing has become a widely adopted slope stabilisation technique for enhancing the structural integrity of soil and rock masses, especially in earthquake and landslide-prone areas. It has effectively stabilised both natural and man-made slopes by preventing erosion, settlement, and other forms of failure, as well as reinforcing existing foundations. In this paper, to investigate the effect of soil nailing on slope stability, a two-dimensional finite element method (2D-FEM) has been used to simulate four different slope conditions: Case-I (no surcharge, no nails), Case-II (surcharge without nails), Case-III (surcharge with nails), and Case-IV (nails without surcharge). This study has introduced a numerical framework that has examined plastic equivalent deviatoric strain, plastic strains along the x- and z-planes, and plastic shear strain to comprehensively assess displacement behaviour under varying conditions. The results have shown significant reductions in displacements along the x-direction (dx), z-direction (dz), and resultant displacement magnitude ($|d|$), particularly in Cases III and IV. Furthermore, the analysis has taken into account several environmental scenarios: (A) without groundwater table (GWT) and seismic loading, (B) with GWT but no seismic loading, (C) without GWT but with seismic loading, and (D) with both GWT and seismic loading. Across all scenarios, the use of soil nails has significantly increased the factor of safety (FOS), whereas increasing the slope angle from 30° to 90° relative to the horizontal plane has resulted in a decrease in FOS, indicating a critical balance between slope inclination and stability. Overall, this study has demonstrated the effectiveness of soil nailing in enhancing slope resilience and has provided comprehensive insights into its performance under diverse environmental and loading conditions.

Keywords: Deviatoric strain, Landslide mitigation, Plastic strain, Slope displacement, Slope stability, Soil nailing

1 Introduction

Soil nailing is a ground improvement technique used to strengthen the soil and/or rock slopes¹⁻³. It involves the installation of reinforcing elements, such as steel bars, into the soil mass to provide additional strength and stability to the soil slope or embankment^{4,5}. It is a simple, fast, and economical construction technique compared to other slope stabilisation techniques⁶. It can be used for both permanent and temporary structures⁶. Soil nails have been extensively used in various geological conditions and are considered an effective slope stabilisation method. They have been applied to stabilise slopes ranging from small residential areas to large highway embankments. This technique is particularly effective in high seismic zones due to its elastic performance, which enhances slope stability and retard slope failure⁷. The primary advantage of soil nailing is its low cost and minimal environmental impact⁶.

Natural slopes are landforms created by natural geological processes, such as erosion, sediment

deposition, and tectonic activities, rather than human activities. They include hillsides, riverbanks, coastal cliffs, and mountain slopes. These slopes can vary in gradient and stability, and their stability is influenced by factors such as soil type, vegetation, moisture content, and underlying rock structure. Natural slopes are subject to weathering and other environmental conditions, which can lead to natural slope failures like landslides and erosion. The natural slopes are commonly seen in hilly areas as shown in Fig. 1. In

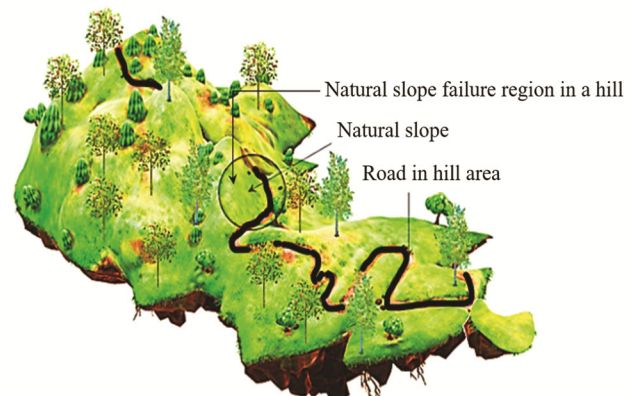


Fig. 1 — Natural slope in hill areas.

*Corresponding author (E-mail: prashant_2k16phdce12@dtu.ac.in)

these areas, the roots in soil slopes (shown in Fig. 2) play a crucial role in stabilising them⁸⁻¹⁰. The function of root reinforcement in natural slopes is multifaceted, providing mechanical and structural benefits that contribute to slope stability and resilience to environmental stresses. The soil structure and methods for slope stabilisation, such as soil nailing, are crucial considerations. Moreover, implementing vegetation planting and constructing retaining walls can also be regarded as effective strategies for enhancing slope stability^{11,12}.

However, with the increasing population and rapid construction, there is a growing need for artificial soil slopes in infrastructure projects such as highways, railways, and other civil engineering structures¹³. The absence of natural root reinforcement weakens the soil, increasing the risk of failure of the slope. However, landslides can have a devastating environmental impact, particularly in mountainous

areas, leading to the destruction of land, wildlife and habitats, air and water pollution, destruction of roads and other infrastructure, loss of life, disruption to local economies, soil erosion and destabilisation of slopes¹⁴. The risk of landslides is caused by various factors such as earthquakes, heavy rainfall, volcanic eruptions, human activities, etc.^{15,16}. It is crucial to be aware of the inherent risk of landslides in susceptible areas and to prioritise the construction of buildings and infrastructure to ensure safety, stability, and resilience. To mitigate landslide risks and enhance slope stability, it is essential to implement preventive measures, including thorough soil structure analysis and slope stabilisation techniques¹⁷⁻¹⁹.

The artificial or man-made earth slopes are built for highways, railway embankments, and other civil engineering structures by using soil nailing, as shown in Fig. 3. These nails play an effective role in the soil mass's active and passive zones,

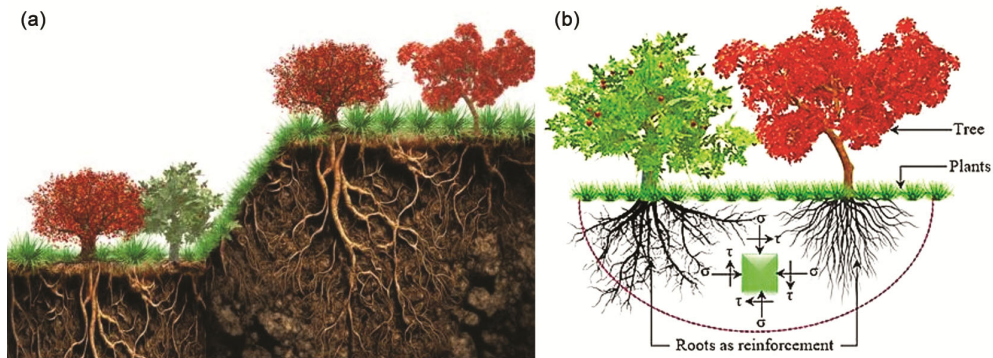


Fig. 2 — Root reinforcement within soil slope (a) Natural root reinforcement, and (b) Function of root reinforcement.

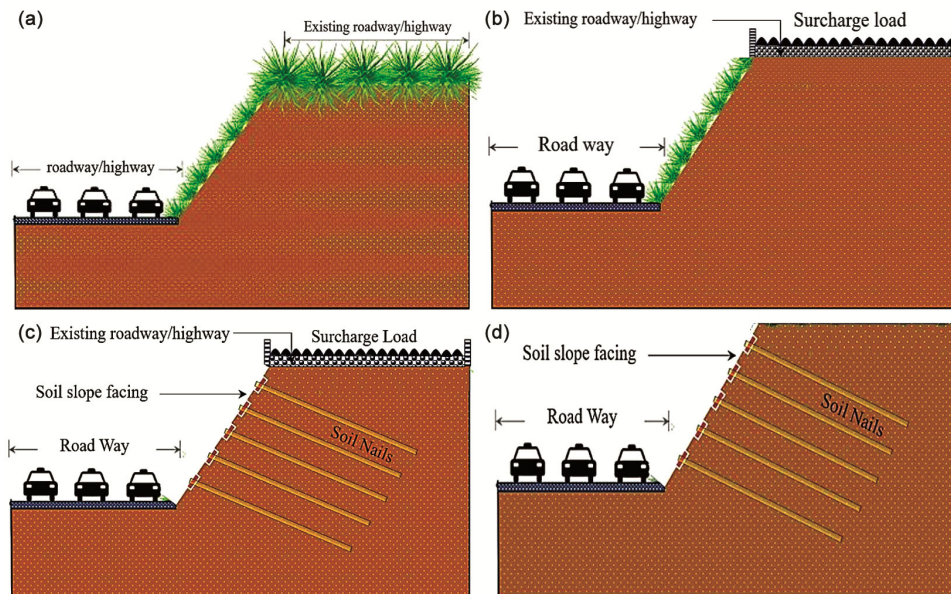


Fig. 3 — Natural/manmade slope for existing roadways/highways (a) Case-I, (b) Case-II, (c) Case-III, and (d) Case-IV

as shown in Fig. 4. The soil nailing technique stabilises a natural slope in hilly areas where the soil is weak and susceptible to landslides²⁰. This technique is often employed on steep slopes or unstable soils, where the risk of landslides is high^{2,17,21}. It is an effective and capable method for stabilising and strengthening slopes, retaining walls, and other existing structures^{6, 22-24}.

Nowadays, soil nailing is increasingly adopted worldwide for the stabilisation of existing structures such as unstable slopes, the construction of new steep slopes or embankments, and retaining walls^{25, 26}. Considering the importance of mitigating landslides and slope failures, this paper emphasises the critical necessity of learning about soil nailing. Accordingly, the analysis in this study was carried out using the FEM alongside analytical techniques implemented in Geo5 software considering the D-P material model. Various essential parameters of soil nails, such as nail length, inclination, diameter, bond strength, and spacing, can be thoroughly analysed by employing numerical modelling. This enables to design and construction of soil nail slopes with enhanced effectiveness and efficiency, leading to more reliable and optimised geotechnical solutions.

Soil nailing has proven to be an effective solution for enhancing the stability of soil slopes by reinforcing the ground and preventing potential failures. Soil nailing has addressed various aspects critical to the stabilisation of soil slopes. Nguyen *et al.* (2023)²⁷ emphasised the significance of spatial variability in influencing slope behaviour, while Rajhans *et al.* (2022)²⁸ provided a comparative evaluation of Limit Equilibrium Methods (LEM) and Finite Element Methods (FEM) for slope stability

analysis. Elahi *et al.* (2022)⁵ investigated the performance of reinforced slopes, and Filho *et al.* (2022)²⁹ examined the behaviour of instrumented soil-nailed walls in Salvador under different environmental conditions. Liu *et al.* (2020)³⁰ introduced a novel Finite Element Limit Equilibrium Method (FELEM) aimed at improving slope stability predictions, whereas Rashid *et al.* (2013)²⁴ evaluated the reinforcing effects of soil nails on slope behaviour.

Several researchers, including Ersoy *et al.* (2020)³¹, He *et al.* (2019)³², He *et al.* (2023)³³, Lazorenko *et al.* (2020)³⁴, Nasvi and Krishnya (2019)³⁵, Qin and Zhou (2023)²⁰, Sari (2022)²¹, Sazzad *et al.* (2016)³⁶, Su and Shao (2021)³⁷, and Wang *et al.* (2021)³⁸, etc., have utilised numerical approaches such as Finite Element Method (FEM) through FLAC 2D and PLAXIS 2D, Finite Element Limit Analysis (FELA), and the Finite Difference Method (FDM) to model and analyse slope stability under various conditions. These studies have contributed significantly to the development of computational models for assessing slope behaviour and the effectiveness of soil nailing techniques. In addition, investigations by Ahmad *et al.* (2023)³⁹, Ahmadi and Borghei (2018)⁴⁰, Li and Xiao (2023)⁴¹, Ng *et al.* (2022)⁴², Pinyol *et al.* (2022)⁴³, Sumartini *et al.* (2021)⁴⁴, Zhou and Qin (2023)⁴⁵, Ramteke and Sâhu (2024)⁴⁶, etc. have focused on understanding failure mechanisms, deformation characteristics, and stability-influencing factors such as surcharge loads, seismic actions, and variations in soil properties. These studies have enhanced the understanding of slope performance under both static and dynamic loading conditions, highlighting the complex interplay of geotechnical parameters.

Despite these advancements, existing studies have largely focused on global stability metrics, with limited emphasis on the internal deformation behaviour of slopes. Addressing this breach, the present study investigates critical displacement factors, including plastic equivalent deviatoric strain, plastic strain along the principal planes, and plastic shear strain, by employing the D-P material model within a 2D-FEM framework. Accordingly, further analyses have been performed to investigate the effects of different scenarios on the stability of soil slopes. This approach aims to provide a more comprehensive understanding of soil slope behaviour and the stabilising effects of soil nails, contributing valuable insights for future slope stabilisation designs and analyses.

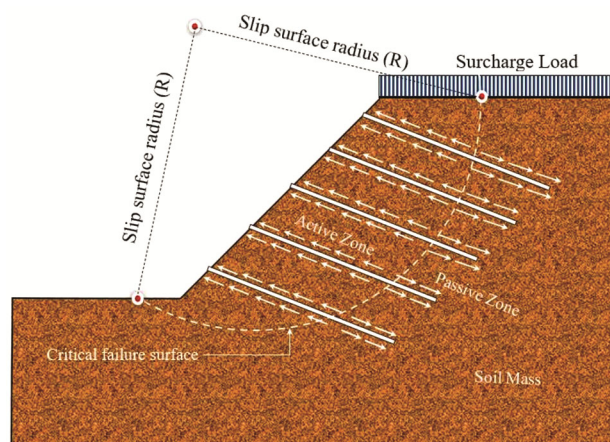


Fig. 4 — Soil-nailed slope phenomenon under surcharge loading.

Landslides are recognised globally as major geological hazards, often triggered by intense rainfall, geological discontinuities, and human activities. Rainfall-induced landslides, in particular, arise from complex interactions among soil properties, hydrological conditions, and topography, leading to significant environmental degradation, sediment discharge, infrastructure damage, and loss of life. In the Indian context, the diversity in climatic and geological settings makes the country especially vulnerable to landslide occurrences. Approximately 12.6% of India's land area, excluding snow-covered regions, is prone to recurrent landslides⁴⁷. Highly susceptible zones include the North-Eastern Himalayas, North-Western Himalayas, the Western Ghats, and the Eastern Ghats, which experience elevated landslide activity, particularly during the monsoon season. Intense rainfall during this period accelerates slope failures, especially in the rugged Himalayan terrain and along the steep escarpments of the Western Ghats. Besides precipitation, sporadic but devastating events such as the 2013 Kedarnath disaster and seismic activities in regions like Sikkim have further highlighted the multifactorial nature of landslides in India⁴⁷. Given the vulnerability mapped across various regions/Indian states (illustrated in Fig. 5), soil nailing emerges as a promising technique for slope stabilisation. By reinforcing the soil mass, soil nails significantly enhance the strength of slopes, mitigate earthquake-induced lateral displacements, and provide additional resistance against rainfall-triggered failures etc^{7,48}. Furthermore, soil nailing offers a cost-effective, adaptable, and energy-dissipating solution to safeguard infrastructure and human lives in landslide-prone areas. Its strategic application could substantially reduce the adverse impacts of seismic activities and extreme rainfall events across India's diverse geographies.

In India, states situated in the northernmost Himalayan regions, including J&K, Himachal Pradesh and Uttarakhand, are highly susceptible to landslide due to their heightened susceptibility. Many districts within these states, characterised by dense populations, face considerable exposure to landslides, impacting vital pilgrimage routes and tourist destinations. Conversely, despite facing numerous landslides annually, the North Eastern states exhibit lower vulnerability socioeconomically due to sparse population densities and vast mountainous areas⁴⁷. The Western Ghats, notably Kerala, face elevated

vulnerability to landslides due to high population and household densities compared to the Himalayan regions. Geographically, landslides are influenced by factors such as the composition of shale-sandstone-metasediments, resulting in dissected hills and valleys with slopes ranging from 30° to 45° across the Himalayas⁴⁷. Rainfall ranging between 750–1000 mm further heightens landslide occurrences⁴⁷. The Chenab sub-basin, characterised by steep mountains, records the highest number of landslides. Although landslides occur on the steep escarpments of the Western Ghats, they are primarily influenced by soil cover on the slopes.

Considering the above facts, the present analysis highlights the essential contribution of soil nails in enhancing slope stability by reducing displacement and controlling deformation. Surcharge loading significantly affects slope behaviour, and the integration of soil nails has been shown to improve resistance to both deformation and failure across the four evaluated scenarios (Case-I to Case-IV). These results provide important insights for designing resilient and sustainable slope stabilisation systems, particularly in regions vulnerable to recurring landslides. In this context, a comprehensive investigation has been carried out, analysing soil slopes with varying inclinations – from 30° to 45°, and steeper angles such as 60° and 90°. The detailed implications of these findings and their results are discussed in the subsequent section.

2 Materials and Methods

The study involves a detailed analysis of soil slope behaviour using appropriate techniques to assess and ensure stability. This research employs geotechnical engineering principles while considering structural integrity and utilising the FEA technique. The design process involves the selection of soil nails and the design of a reinforcement system based on anticipated loading conditions. The analysis focuses on evaluating the response of the soil nailed slope under surcharge loading, examining ground movements and failure mechanisms (i.e. FOS). The FOS is computed for the specific soil slope conditions. This design philosophy contributes to the field of slope stabilisation by providing an effective and efficient approach utilising soil nailing. The study offers valuable insights into the design and implementation of slope stabilisation measures.

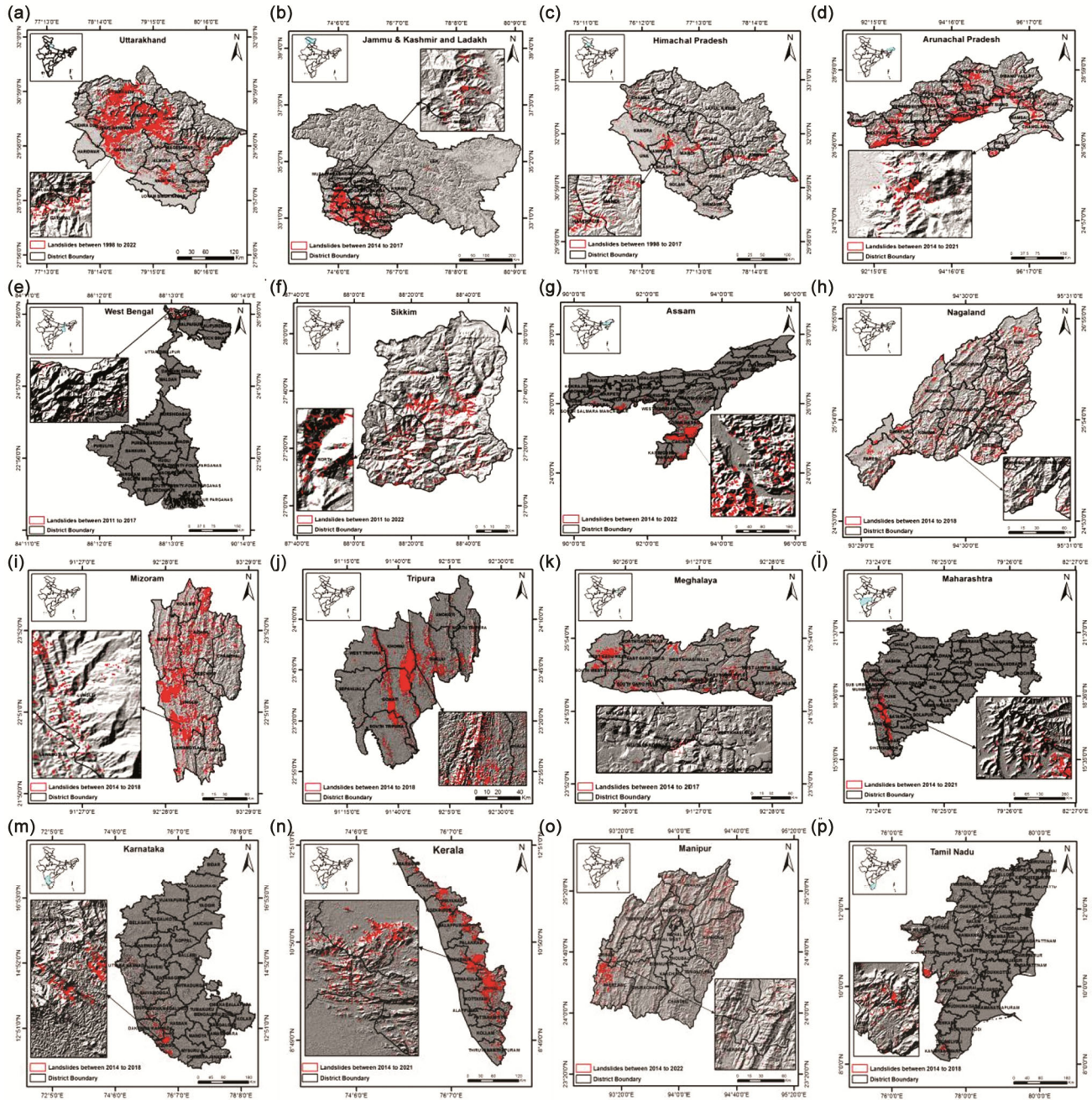


Fig. 5 — Landslides were mapped using high-resolution satellite data in different states of India, which occurred between 1998 to 2022. (a) Uttarakhand, (b) Jammu & Kashmir and Ladakh, (c) Himachal Pradesh, (d) Arunachal Pradesh, (e) West Bengal, (f) Sikkim, (g) Assam, (h) Nagaland, (i) Mizoram, (j) Tripura, (k) Meghalaya, (l) Maharashtra, (m) Karnataka, (n) Kerala, (o) Manipur and (p) Tamil Nadu ⁴⁷.

In this investigation, the model's input parameters include the angle of internal friction (ϕ), Poisson's ratio (ν), modulus of elasticity (E), and cohesion (c), which define the yield condition. Additionally, effective parameters such as effective cohesion (c_{eff}), effective angle of internal friction (ϕ_{eff}), nails

inclination (α) and dilation angle (ψ) are considered. The D–P model, also known as the extended Von Mises model, modifies the Mohr–Coulomb yield function to eliminate singularities associated with corners (Geo5, 2018). The yield surface forms a smooth cylindrical cone in principal stress

space, with its projection in the deviatoric plane touching the inner corners of the Mohr–Coulomb hexagon ($\theta = -30^\circ$), as shown in Fig. 6, where θ represents the Lode angle (Geo5, 2018). Figs. 6 and 7 illustrate the yield surfaces of Drucker–Prager and Mohr–Coulomb, respectively.

The 2D-FEM is a widely used numerical technique for solving soil-nailed slope stabilisation problems. It has also been used to analyse the stability of soil-nailed slopes under various loading conditions such as seismic, static and dynamic loading, etc.⁴⁹. FEM is a numerical approach widely used to analyze complex physical phenomena, as demonstrated in studies by Zhao and Shao (2008)³⁴; Sazzad *et al.* (2016)³⁶; Chakrabarti and Shivananda (2019)⁵⁰; Lazorenko *et al.* (2020)⁵¹.

In this study, the behaviour of a soil-nailed slope is analysed using 2D-FEM. The investigation utilizes a soil slope model, illustrated in Fig. 8, which highlights two distinct interfaces, namely Interface-I and Interface-II. The corresponding soil properties for

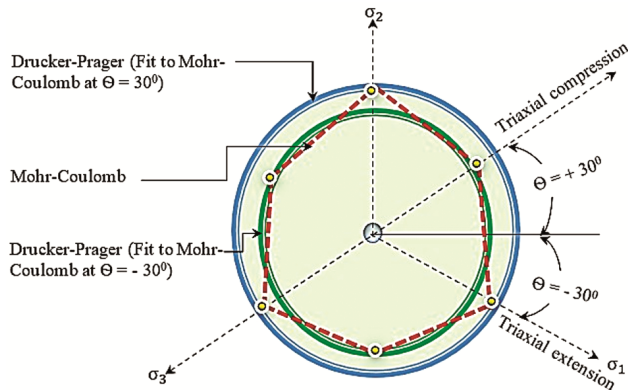


Fig. 6 — Deviatoric plane yield surfaces: Drucker-Prager versus Mohr-Coulomb Models (Geo 2018).

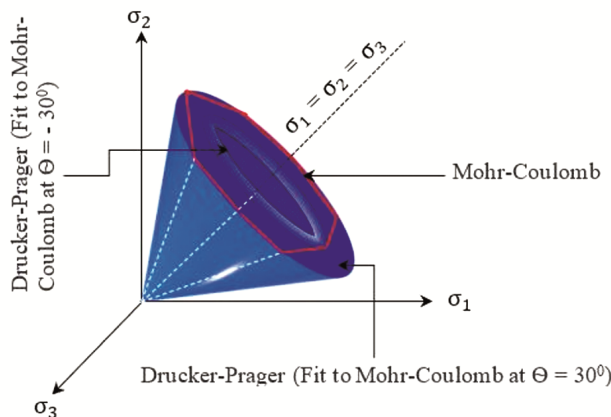


Fig. 7 — Yield surface Drucker-Prager and Mohr-Coulomb (Geo5, 2018).

these interfaces are detailed in Table 1. The soil is then idealized as a two-dimensional plane element using the D-P elastoplastic soil model. Geo5 (2018) Fine software is used to perform the analysis, generating a finite element mesh with 7111 nodes and 3922 elements including 2994 regions, 232 beams, and 696 interfaces, shown in Fig. 9. The materials and their properties used in this analysis are demonstrated in Table 1.

3 Results and Discussion

This study aims to examine the behaviour of a slope in various scenarios to enhance the understanding of optimal design and construction for ensuring user safety. The behaviour of the slope is influenced by

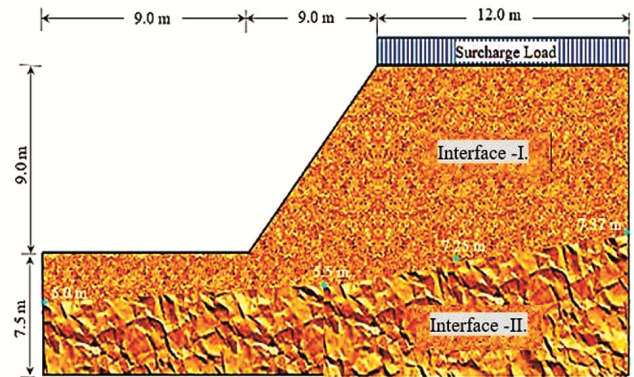


Fig. 8 — Model used for finite element analysis (distinct with two interfaces).

Table 1 — Properties used for analysis (Soils and Nail).

Properties of Soil	Symbol	Interface-I	Interface-II
		Drucker-Prager	
Surcharge Load (kN/m^2)	(q)	35	
Unit weight (kN/m^3)	(γ)	18.00	20.00
Poisson's ratio	(ν)	0.30	0.20
Elastic modulus (MPa)	(E)	21.00	30.00
Modulus unloading/reloading (MPa)	(E_{ur})	21.00	30.00
Angle of internal friction ($^\circ$)	(ϕ_{ef})	23.00	38.00
Cohesion of soil (kPa)	(c_{ef})	9.00	12.00
Dilation angle ($^\circ$)	(ψ)	0.00	0.00
Saturated unit weight (kN/m^3)	(γ_{sat})	20.00	22.00
Properties of Nail			
Length of nail (m)	(L)	9.00	
Nail inclination with horizontal ($^\circ$)	(α)	15	
Diameter of the nails (mm)	(ϕ)	30	
Elastic Modulus (N/mm^2)	(E)	2×10^5	
Nail Spacing (m)	(b)	1.00	

factors such as the type of soil, slope angle, and size and quantity of installed nails. The findings will enable users to comprehend the risks associated with these different cases and to make informed decisions, potentially necessitating enhanced safety measures in the presence of a surcharge. From this perspective, an analysis of soil slope characteristics has been conducted to provide deeper insights, as discussed in the following paragraph.

3.1 Identification of displacement in x and z-direction

By leveraging the 2D-FEM for displacement analysis, valuable insights into the behaviour of the

system can be gained. FEM breaks down complex problems into simpler components and solves them numerically, allowing for a detailed examination of the system's response. Studying the displacement data produced by FEM provides a comprehensive understanding of the system's behaviour and identifies potential areas for improvement.

From the analysis examining (refer to Fig. 10) Case-I, the analysis reveals that the maximum soil displacement along the x- and z-planes (d_x , d_z) measures at 10.00 mm and 7.306 mm, respectively, resulting in a combined displacement of 10.1 mm, as depicted in the vector diagram in Fig. 10. In Case-II, the displacement along the x- and z-planes increases to 25.8 mm and 18.7 mm, respectively, resulting in a combined displacement $|d|$ of 27.8 mm, as illustrated in Fig. 11. Similarly, in Case-III, the displacement along the x- and z-planes decreases to 18.2 mm and 14.1 mm, respectively, resulting in a combined displacement $|d|$ of 18.8 mm, as depicted in Fig. 12. This output underscores the added resistance to displacement offered by Case-III. However, considering Case-IV, the displacement along the x- and z-planes notably decreases to 7.5 mm and 6.75 mm, respectively, resulting in a combined displacement $|d|$ of 9.4 mm, as shown in Fig. 13. The

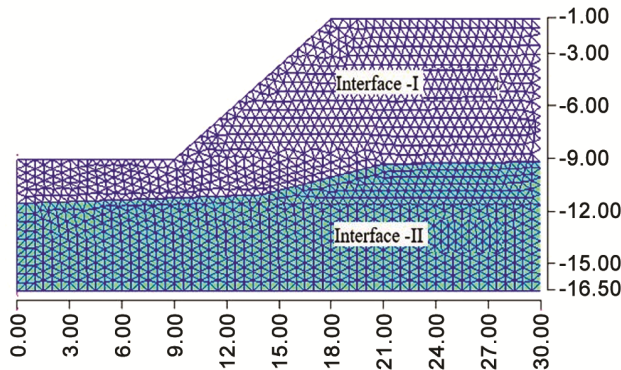


Fig. 9 — Finite element model with two Interfaces.

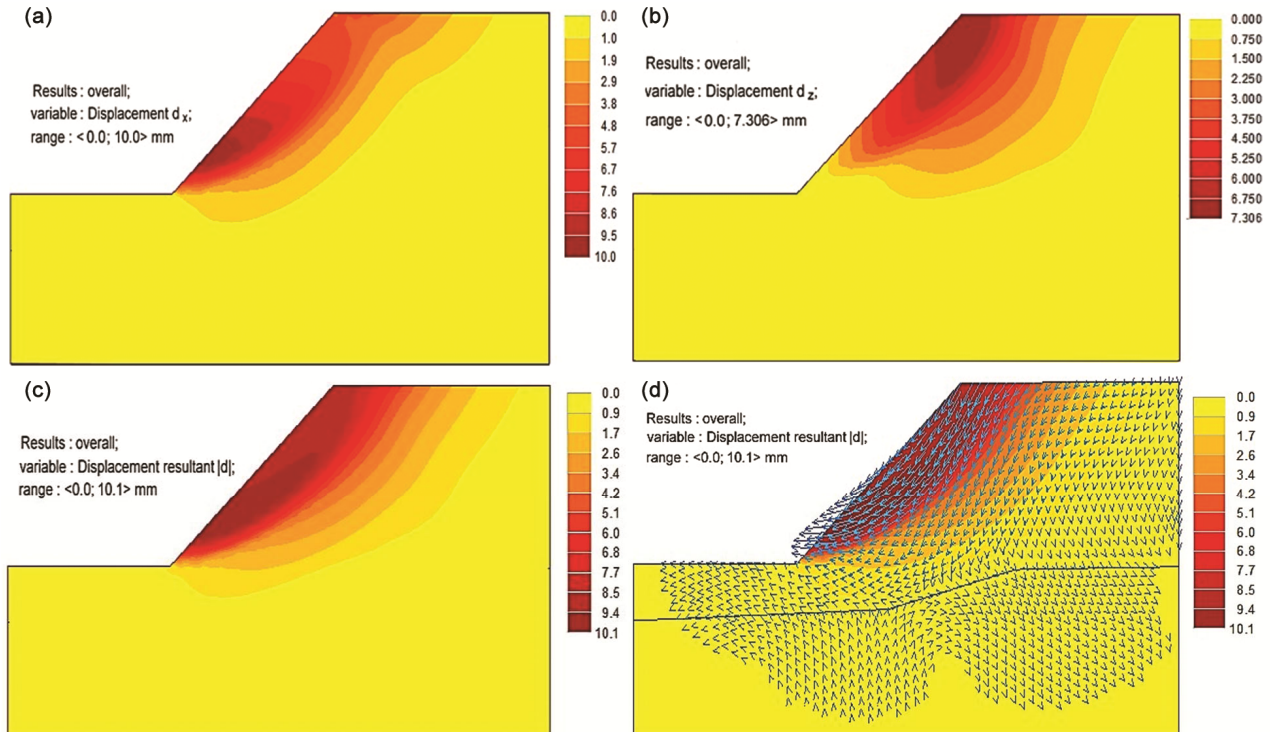


Fig. 10 — Displacement of soil slope in Case – I: (a) Displacement (d_x), (b) Displacement (d_z), (c) Displacement resultant $|d|$ and (d) Vector diagram - displacement resultant $|d|$.

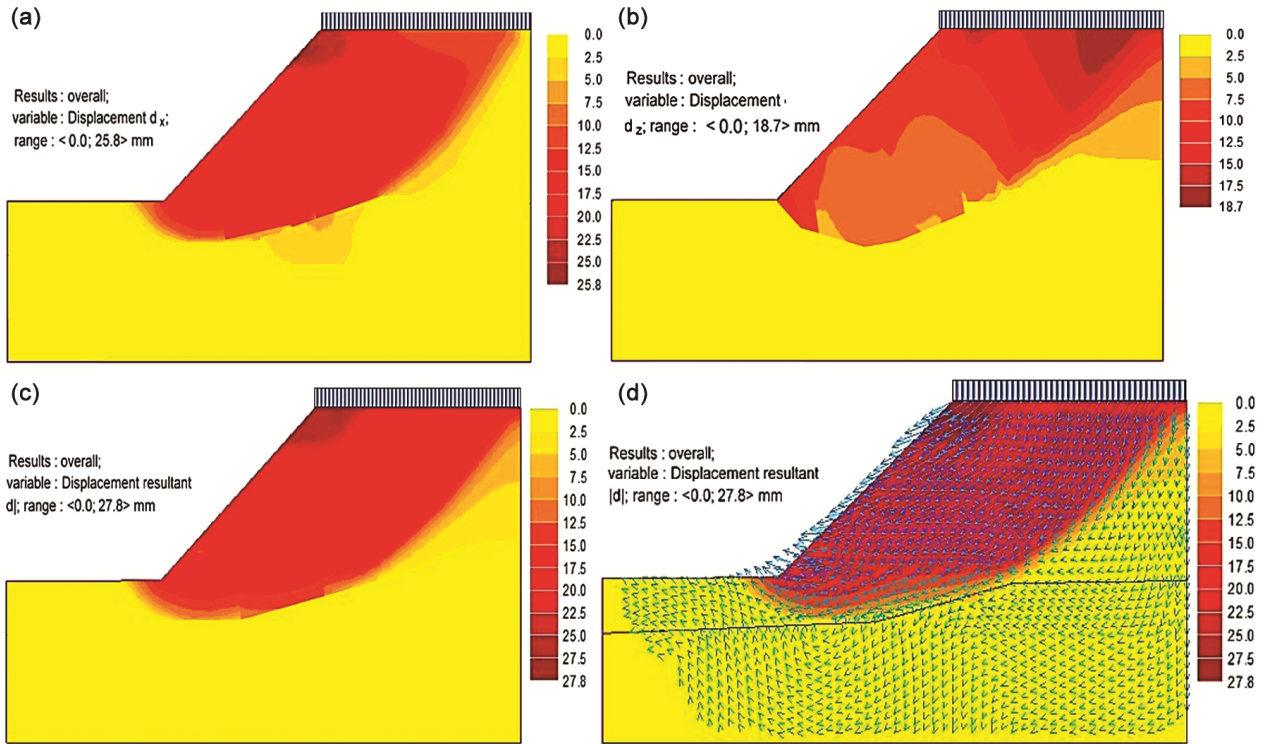


Fig. 11 — Displacement of soil slope in Case – II: (a) Displacement (dx), (b) Displacement (dz), (c) Displacement resultant |d| and (d) Vector diagram - displacement resultant |d|.

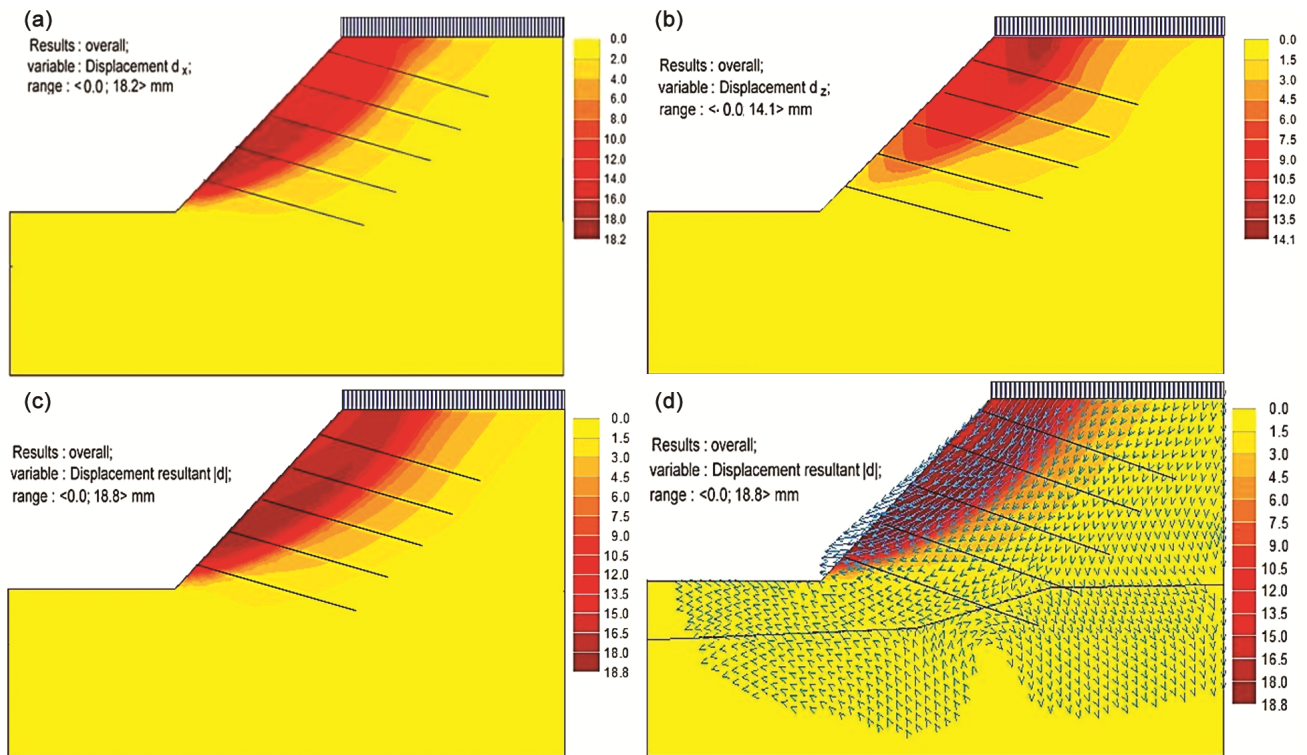


Fig. 12 — Displacement of soil slope in Case – III: (a) Displacement (dx), (b) Displacement (dz), (c) Displacement resultant |d| and (d) Vector diagram - displacement resultant |d|.

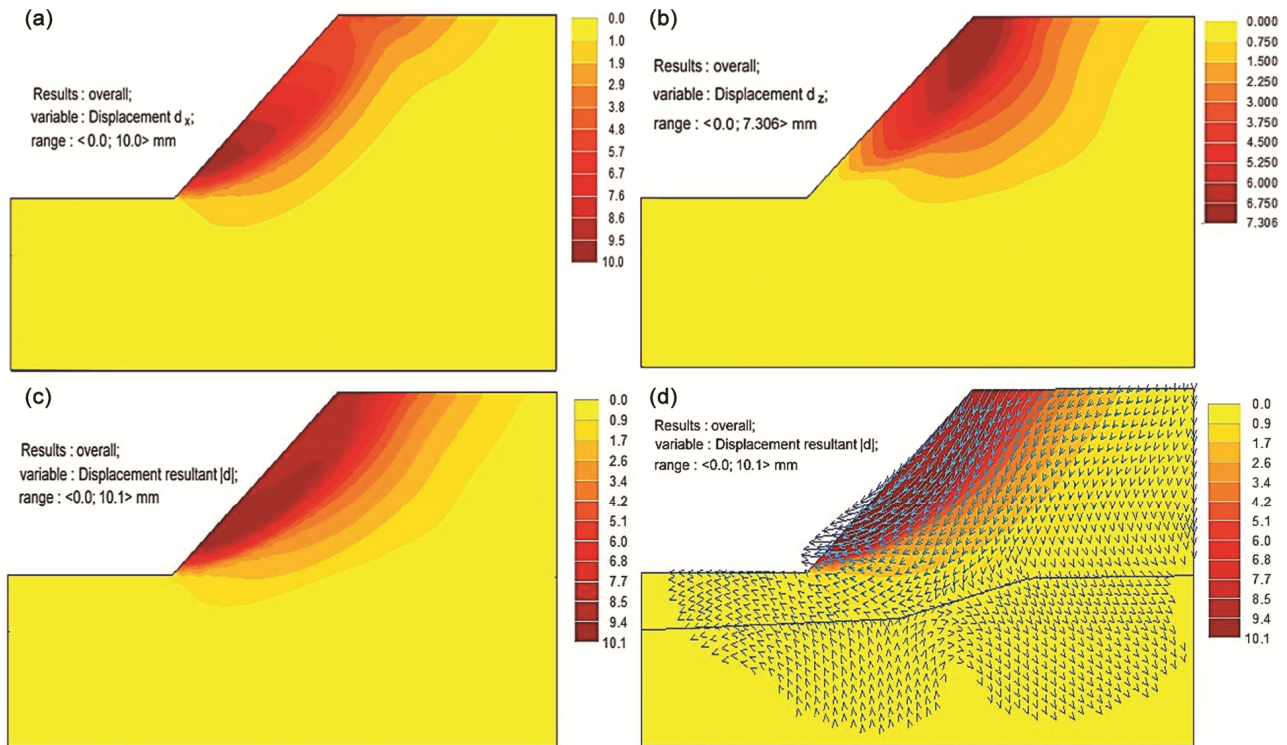


Fig. 13 — Displacement of soil slope in Case – IV : (a) Displacement (d_x), (b) Displacement (d_z), (c) Displacement resultant $|d|$ and (d) Vector diagram - displacement resultant $|d|$.

comparative analysis reveals that soil nails contribute significantly to reducing displacement in both x-plane (d_x) and z-plane (d_z) orientations, as well as the resultant displacement $|d|$, indicating their effectiveness in stabilizing soil slopes. Without a surcharge load, soil nails reduce x-direction displacement by 25% and z-direction displacement by approximately 7.63%. Under surcharge load conditions, the reduction in displacement is more pronounced, with soil nails decreasing x-direction displacement by approximately 28.63% and z-direction displacement by about 24.60%. In terms of resultant displacement $|d|$, the reduction is approximately 6.93% without a surcharge load and a substantial 32.37% under surcharge load conditions. These findings underscore the importance of soil nails in enhancing slope stability, particularly in mitigating the effects of external loads like surcharge loads.

3.2 Plastic equivalent deviatoric strain ($E_{d,pl}$)

It is important to note that the plastic equivalent deviatoric strain ($E_{d,pl}$) in a soil slope is affected by the type of soil, the magnitude of the applied load, the existing soil parameters, etc.⁵². Hence, this can be used to evaluate the stability of a soil slope under

various conditions. The plastic equivalent deviatoric strain of the soil slope will increase under the surcharge load. However, the exact amount of increase will differ based on the conditions of the soil slope⁵³.

In the present study, the analysis in Fig. 14 demonstrates that the inclusion of soil nails has a notable impact on the plastic equivalent deviatoric strain of the soil slope. By reinforcing the shear strength of the soil and enhancing slope stability, the presence of nails contributes to this effect. The comprehensive simulation results of the plastic equivalent deviatoric strain, obtained through FEM, are visually presented in Fig. 14. In this study, the plastic equivalent deviatoric strain is observed 2.73%, 4.35%, 2.64% and 1.70% for Case-I, Case-II, Case-III and Case-IV respectively. The performance of soil slopes in each scenario has been evaluated comprehensively by assessing the percentage of utilization of plastic equivalent deviatoric strain, as demonstrated in Fig. 15. It is notable that under surcharge load without soil nails (Case-II), the contribution to plastic equivalent deviatoric strain is significantly higher (i.e. 38%) compared to other cases, while the least contribution (i.e. 15%) is

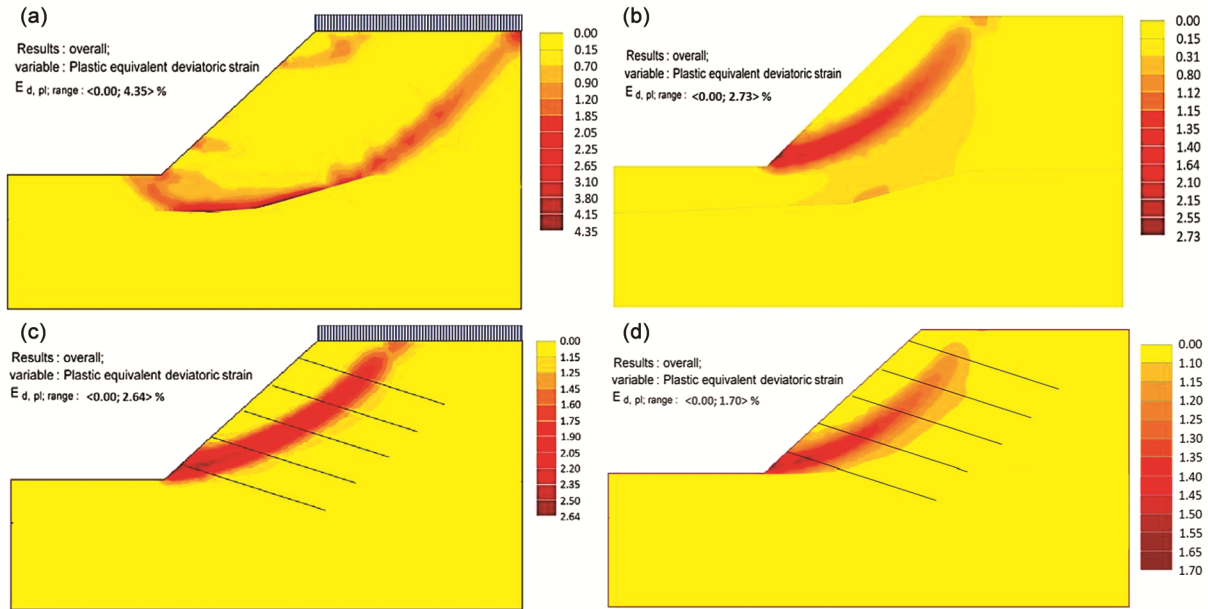


Fig. 14 — Plastic equivalent deviatoric strain (a) Case-I, (b) Case-II, (c) Case-III and (d) Case-IV.

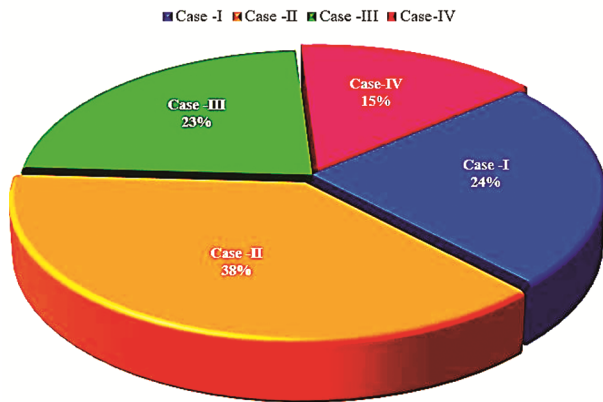


Fig. 15 — Percentage contribution of plastic equivalent deviatoric strain ($E_{d,pl}$) in each case.

observed in Case-IV, which represents a soil-nailed slope without surcharge loading. It is important to highlight that the presence of soil nails within the slope results in a significant reduction in plastic equivalent deviatoric strain, as demonstrated by this comparative analysis (refer to Fig. 15).

3.3 The plastic strains in soil slope

The plastic strain observed in a soil slope is primarily influenced by the strength characteristics of the soil, the magnitude and distribution of the surcharge load, and the presence of soil nails⁵⁴. These factors collectively determine the strain experienced by the soil mass. When soil nails are introduced into

the slope, they play a crucial role in distributing the load more efficiently^{55,56}. Soil nails act as reinforcing elements that enhance the overall stability and load-bearing capacity of the slope^{6,57}. The inclusion of soil nails serves as a strategic measure to distribute strain more evenly across the soil mass, effectively alleviating the concentrated strain points and thereby reducing the potential for plastic deformation within the soil structure. Referencing Fig. 16 for insights into the x-plane observations and Fig. 17 for those concerning the z-plane, we can distinguish the impact of different cases on plastic strain behaviour. In Case-I, the plastic strain in the x-plane ranges from below 0.00 to just over 1.00%, while in Case-II, it extends to approximately 1.39%. Moving to Case-III, the range diminishes to below 0.00 to about 0.88%, and in Case-IV, it further reduces to below 0.00 to around 0.49%. Similarly, in the z-plane, Case-I exhibits a minimum plastic strain of below 0.00 to approximately 0.484%. In Case-II, it is comparable, ranging from below 0.00 to about 0.49%. As for Case-III, the plastic strain lessens to below 0.00 to approximately 0.46%, and in Case-IV, it decreases even further to below 0.00 to about 0.32%. These findings, as illustrated in the accompanying Fig. 16 and Fig. 17, underscore the efficacy of soil nails in managing plastic strain across different scenarios, thereby enhancing structural stability and resilience. Fig. 18 provides a graphical representation of the plastic strains observed along the x and z planes for

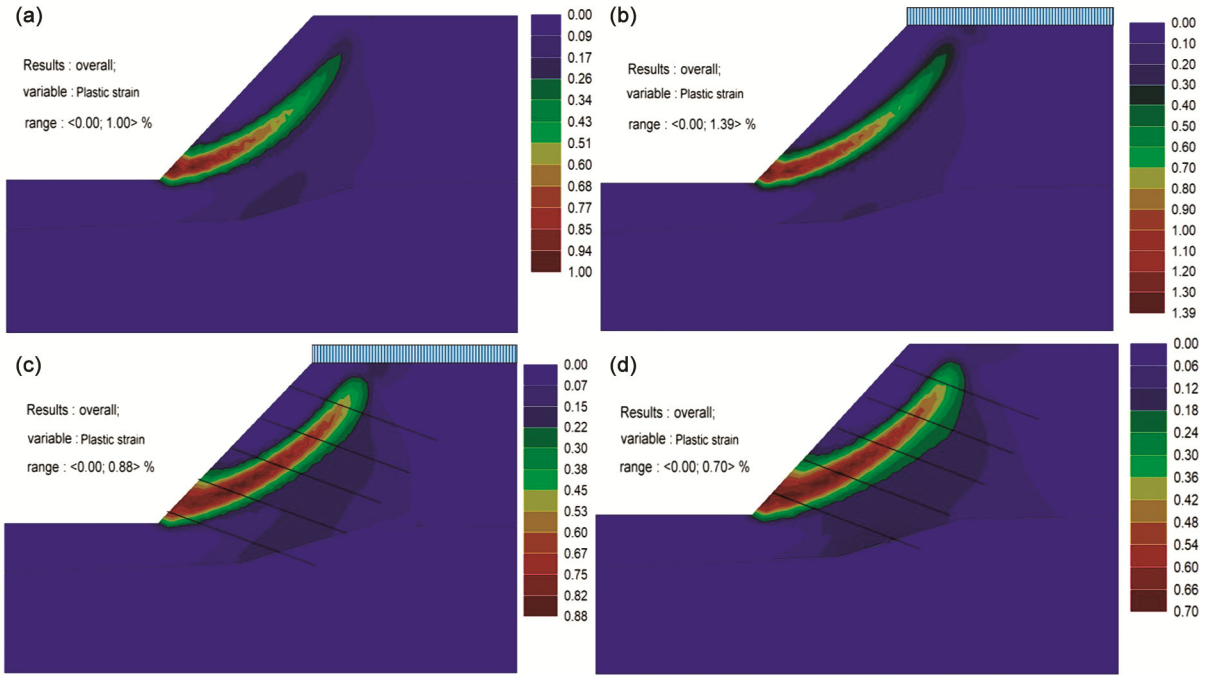


Fig. 16 — Plastic strain about x-plane: (a) Case-I, (b) Case-II, (c) Case-III and (d) Case-IV.

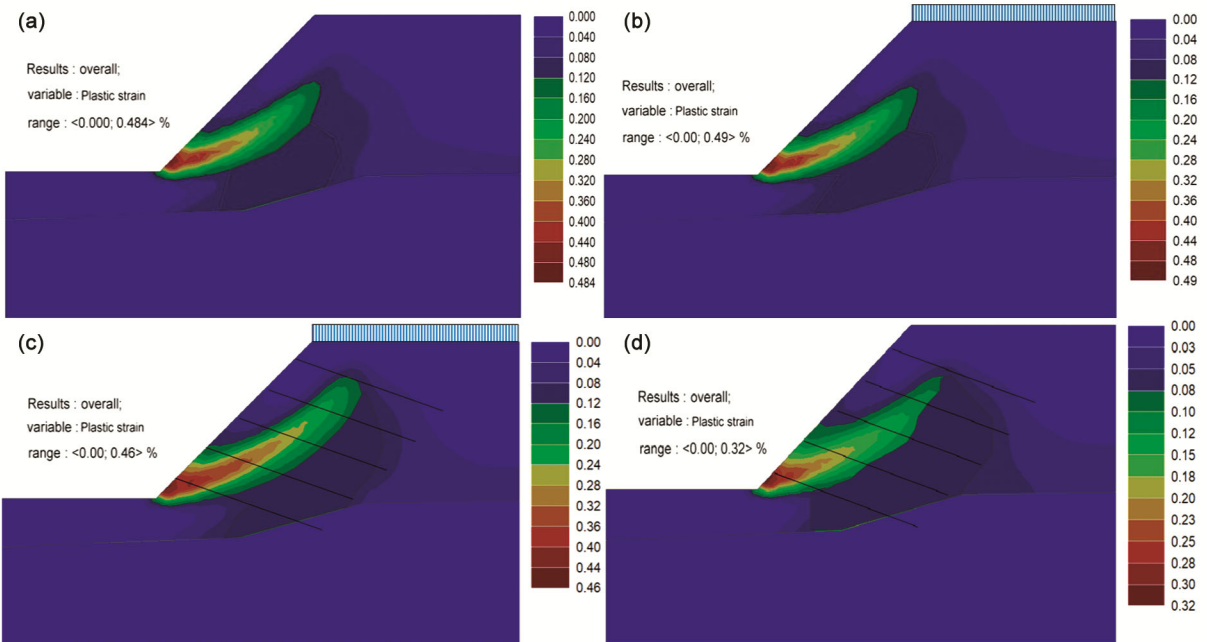


Fig. 17 — Plastic strain about z-plane: (a) Case-I, (b) Case-II, (c) Case-III and (d) Case-IV

different cases. This visualization allows for a better understanding of the variation in plastic strain distribution across the slope under different circumstances. It showcases the impact of soil nails on reducing plastic strain and improving the overall performance and stability of the soil slope compared to the other cases.

3.3.1 Plastic shear strain in soil slope

Plastic shear strain is an important parameter when studying the deformation characteristics and potential failure mechanisms of soil slopes^{58, 59}. It provides insights into the shear deformation and potential instability of the slope material. However, assessing plastic shear strain requires considering other factors

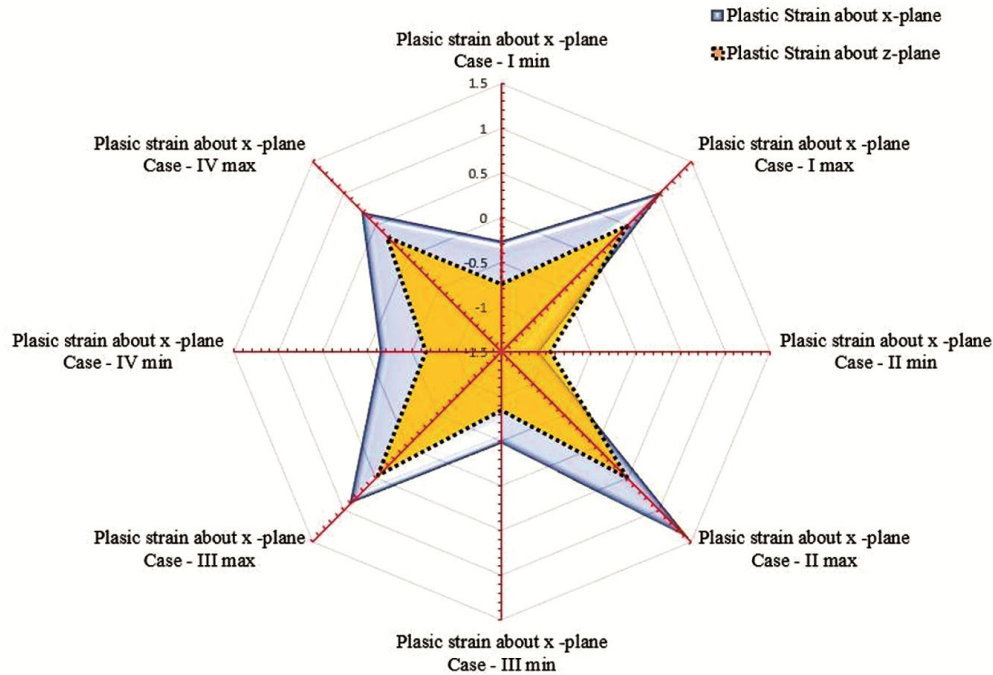


Fig. 18 — Graphical representation of the plastic strain in soil slope about x-plane and z-plane.

such as shear strength parameters, safety factors, and comprehensive slope stability analysis to fully evaluate slope stability⁵⁹. In this study, to examine plastic shear strain within a soil slope, four distinct cases were investigated: Case-I, Case-II, Case-III, and Case-IV. Each case was characterised by its unique set of parameters and inputs. Case-I focused on analysing soil properties and slope angle, while Case-II expanded the scope to include soil properties, surcharge load, and slope angle considerations. Moving forward, Case-III delved into a more comprehensive analysis, encompassing soil properties, surcharge load, and the outline of soil nails. Finally, Case-IV examined the impact of soil nails in the absence of surcharge, among other factors. The output of the 2D-FEM analysis yielded valuable insights into the distribution of plastic shear strain across each case, as visually represented in Fig. 19.

Observations from Fig. 19 reveal that in Case-I, plastic shear strain ranged from 0.00% to a maximum of 1.39%. Similarly, in Case-II, the strain varied from 0.00% to a maximum of 1.48%. Case-III exhibited plastic shear strain values ranging from 0.00% to a maximum of 1.20%, while Case-IV ranged from 0.00% to a maximum of 1.10%. Notably, Case-III and Case-IV displayed the lowest recorded values of plastic shear strain, attributed to the presence of soil nails within the soil mass and the restraint they afford. To

visually illustrate the utilisation of plastic shear strain across the entire model for the different cases, refer to Fig. 19 and Fig. 20. These figures provide clear representations of the distribution and magnitude of plastic shear strain (%) throughout the slopes.

3.3.2 Plastic volumetric strain in soil slope

Plastic volumetric strain is important in studying soil slopes as it helps us understand the extent of deformation occurring within the soil slope⁶⁰. By quantifying the changes in volume caused by plastic deformation, we can identify potential failure mechanisms and assess the stability of the slope. Additionally, plastic volumetric strain provides insights into the effectiveness of stabilisation measures and helps us understand how soils behave when subjected to deformation. Its role in assessing deformation, analysing failures, evaluating stability, considering design aspects, and understanding soil behaviour makes plastic volumetric strain a crucial parameter in the study of soil slopes. The plastic volumetric strain in a soil slope is influenced by various factors and can differ depending on the presence of a surcharge load and soil nails⁵⁵. In Case-I, the plastic volumetric strain primarily responds to gravitational loading. It increases with the slope angle and soil type while decreasing with the soil cohesion and internal friction angle. Case-II, on the other hand,

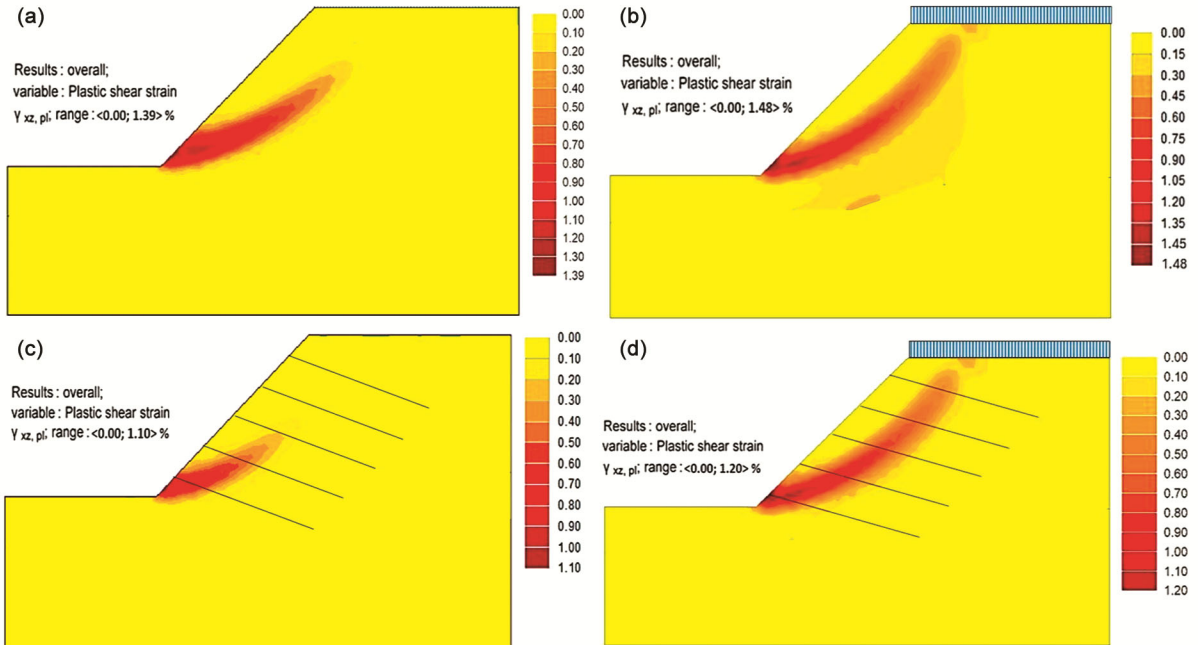


Fig. 19 — Plastic shear strain: (a) Case-I, (b) Case-II, (c) Case-III and (d) Case-IV.

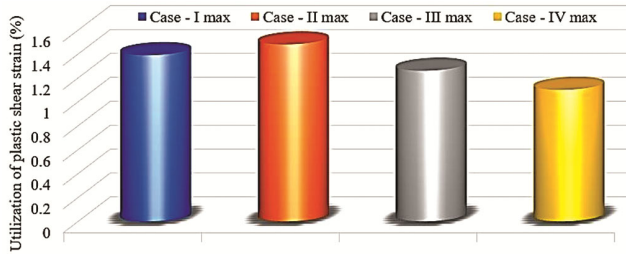


Fig. 20 — Utilization of plastic shear strain in the whole model.

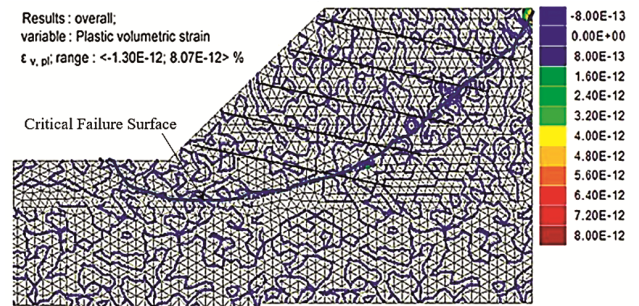


Fig. 21 — Plastic volumetric strains in the entire soil slope.

involves both surcharge and gravitational loading, resulting in increased plastic volumetric strain with higher slope angle, surcharge load, and soil type, while decreasing the soil cohesion and internal friction angle. In Case-III, the plastic volumetric strain is affected by the surcharge, gravitational loading, and additional loading and restraint provided by the soil nails. Whereas in Case-IV, plastic volumetric strain is affected by soil nails within the slope. As a result, it increases with the slope angle, surcharge load, and soil type, and decreases with the presence of soil nails, soil cohesion, and internal friction angle. Figure 21 illustrates the distribution of plastic volumetric strain across the slope, providing a visual representation of deformation behaviour. Understanding plastic volumetric strain is essential for evaluating the deformation characteristics and potential failure mechanisms of soil slopes, taking into account factors such as slope angle, surcharge

load, soil type, cohesion, internal friction angle, and the inclusion of soil nails. Building on this understanding, further investigations have been conducted to assess the effects of the groundwater table (GWT) and seismic loading on slope stability across different slope geometries.

3.4 GWT and Seismic Effect on Soil Slope Stability Considering Different Slopes Geometry

As defined above soil slopes phenomenon, in this study, slope stability was scientifically assessed using Geo5 software across a range of geometric configurations, incorporating variations in slope inclination, the inclusion of soil nails, and the influence of both groundwater table (GWT) conditions and seismic loading (Fig. 22). The investigation encompassed multiple scenarios (A to D), with a focus on important geotechnical parameters

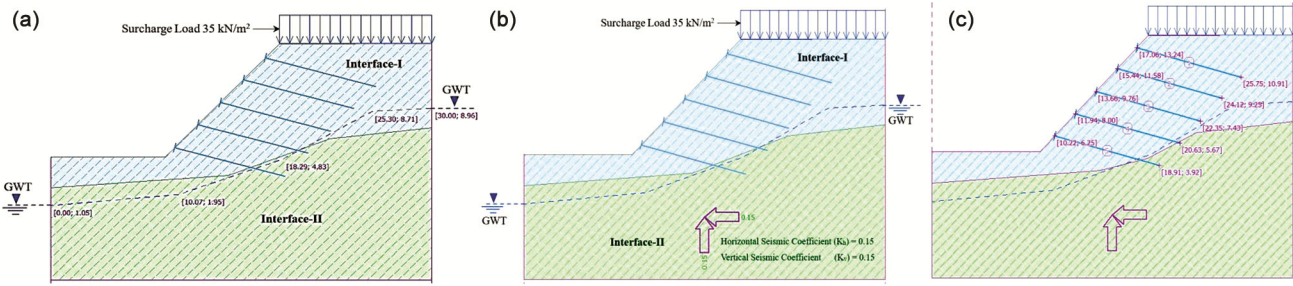


Fig. 22 — Soil slope geometry considerations (a) Groundwater table (GWT), (b) Seismic coefficients (K_h & K_v) and (c) a complete model for analysis.

such as soil cohesion (c), internal friction angle (ϕ), and slope angle (Θ). Specific details of GWT levels and seismic coefficients are illustrated in Fig. 22 (a & b), respectively. The FOS values were evaluated for slope angles ranging from 30° to 90° , as detailed in Table 2. Results indicate that the incorporation of soil nails markedly improves slope stability, with FOS values consistently exceeding the FHWA (2003)⁶ recommended minimum of 1.5, thereby highlighting their effectiveness in reducing landslide susceptibility. The FOS data were further examined through box plot representation (Fig. 23), revealing the distribution and variability across different slope conditions. Additionally, a heatmap analysis (Fig. 24) demonstrated a general decline in FOS with increasing slope angle, underscoring the inverse relationship between slope steepness and stability, and emphasising the importance of design trade-offs in slope reinforcement strategies.

The detailed analysis of FOS under diverse conditions, including the presence of GWT, seismic coefficients (K_h & K_v), soil nails, and surcharge loads at various slope angles (30° , 45° , 60° , and 90°), offers a comprehensive understanding of slope stability dynamics (refer to Fig. 24). The results for different scenarios (A to D) are summarized in Table 2. In scenario (A), which lacks both GWT and seismic coefficients, there is a consistent decrease in stability with increasing slope angles. For instance, Case-I's FOS decreases from 2.02 at 30° to 1.45 at 90° , whereas Case-IV, which includes soil nails without surcharge load, exhibits the highest FOS (2.28 at 30° to 1.82 at 90°), underscoring the stabilising role of soil nails. In scenario (B), which includes GWT but not seismic coefficients, lower FOS values were observed compared to scenario (A). Case-I's FOS ranges from 1.95 at 30° to 1.23 at 90° , highlighting the destabilizing impact of GWT, especially at steeper angles. However, Case-IV maintains relatively stable

Table 2 — Factor of safety (FOS) with different soil slope cases and scenarios.

S No.	Conditions of Soil Slope	Factor of Safety (FOS) for different slope angles (Θ)			
		30°	45°	60°	90°
(A) Soil slope without GWT & without seismic coefficients					
1	Case-I	2.02	1.62	1.59	1.45
2	Case-II	1.69	1.40	1.25	1.24
3	Case-III	1.96	1.76	1.68	1.56
4	Case-IV	2.28	2.07	1.92	1.82
(B) Soil slope with GWT & without seismic coefficients					
1	Case-I	2.95	1.60	1.46	1.23
2	Case-II	1.59	1.25	1.11	1.06
3	Case-III	1.88	1.46	1.39	1.19
4	Case-IV	2.25	1.82	1.61	1.40
(C) Soil slope without GWT & with seismic coefficients					
1	Case-I	1.47	1.12	1.07	1.02
2	Case-II	1.24	0.97	0.90	0.90
3	Case-III	1.37	1.51	1.44	1.16
4	Case-IV	1.56	1.52	1.50	1.24
(D) Soil slope with GWT & with seismic coefficients					
1	Case-I	1.40	1.09	1.01	0.65
2	Case-II	1.05	0.98	0.90	0.60
3	Case-III	1.25	1.16	1.15	1.10
4	Case-IV	1.53	1.49	1.46	1.21

FOS values (2.25 at 30° to 1.40 at 90°), despite the presence of GWT. Scenario (C), which excludes GWT but includes seismic coefficients, shows that seismic forces uniformly reduce stability across all cases. Case-II has the lowest FOS values (1.24 at 30° to 0.90 at 90°), indicating vulnerability to seismic activity without soil nails. Conversely, Cases III and IV, which incorporate soil nails, maintain higher FOS values (Case-III: 1.37 at 30° to 1.16 at 90° ; Case-IV: 1.56 at 30° to 1.24 at 90°), demonstrating the effectiveness of soil nails in mitigating seismic-induced instability. Scenario (D), which encompasses both GWT and seismic coefficients, exhibits the

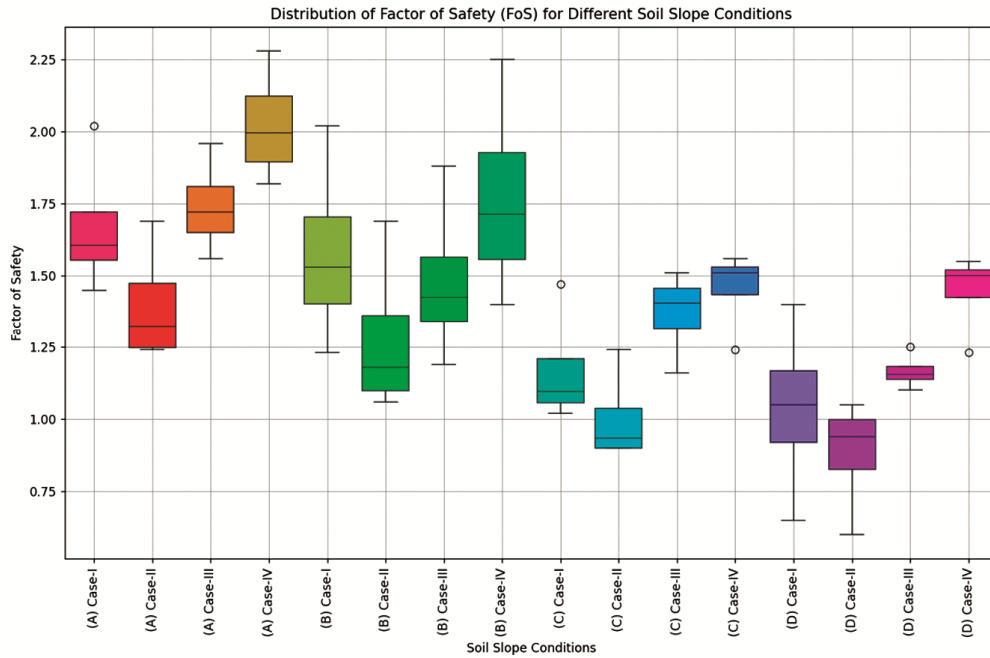


Fig. 23 — Box plot: Distribution of FOS for different soil slope conditions.

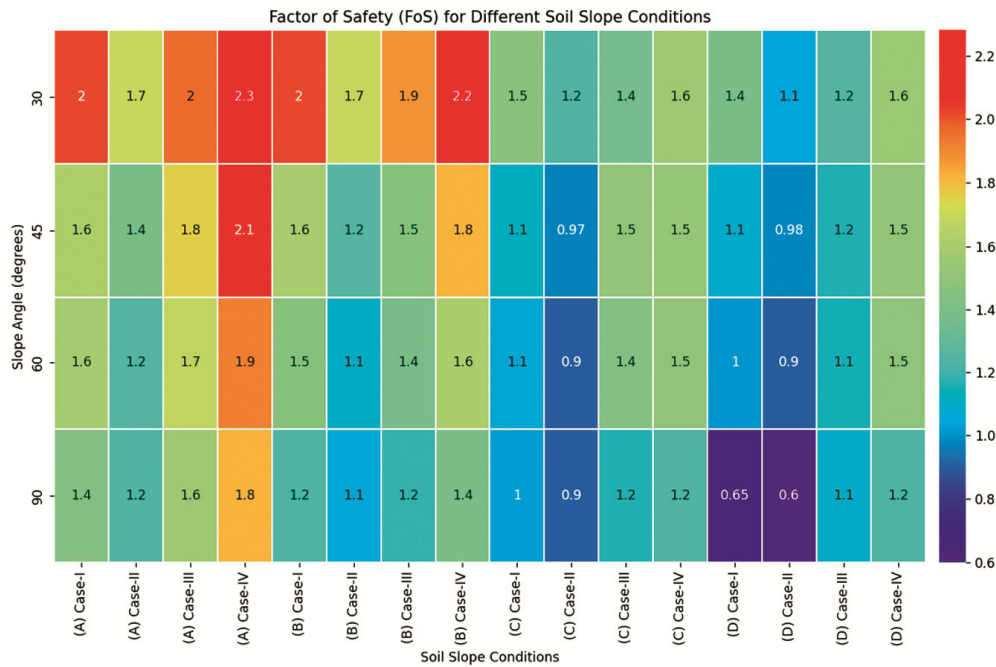


Fig. 24 — Heat Map observation for different soil slope angles and conditions.

lowest overall FOS values. Case-II is particularly unstable (FOS: 1.05 at 30° to 0.60 at 90°), showing high susceptibility to combined destabilizing factors. Remarkably, Case-IV retains the highest FOS values (1.55 at 30° to 1.23 at 90°), highlighting the critical role of soil nails in enhancing slope stability under challenging conditions (see Figs. 23 and 24).

From Fig. 23, we gain key insights into soil slope stability, the distribution of stability levels is clearly demonstrated, showing how the FOS varies across different conditions and angles; the presence of a GWT and seismic coefficients generally reduces stability, as indicated by lower FOS values; soil nails significantly enhance stability, as evidenced by higher

FOS values in scenarios where they are used; and slope angle has a noticeable effect on stability, with steeper angles generally showing lower FOS values, highlighting the increased risk of landslides at steeper slope inclinations (refer to heatmap plot Fig. 24). These visual insights are allowing for more informed decisions regarding stabilisation strategies in landslide mitigation efforts.

Overall, the box plot (Fig. 23) and heatmap (Fig. 24) support understanding the complex interactions between various factors affecting slope stability and guiding effective engineering solutions. The heatmap, generated in this analysis, visually represents the FOS values across different soil slope scenarios (A to D) and slope angles (30°, 45°, 60°, and 90°), with colour intensity reflecting the magnitude of the FOS values. Several key insights are observed: Scenario (A) shows the highest stability without GWT and seismic coefficients, especially in Case-IV with FOS values from 2.28 at 30° to 1.82 at 90°, indicating the effectiveness of soil nails. Scenario (B), with GWT but without seismic coefficients, exhibits a noticeable drop in stability compared to Scenario (A), although Case-IV maintains relatively higher FOS values (2.25 at 30° to 1.40 at 90°), highlighting soil nails' mitigating effect on GWT's destabilizing influence. Scenario (C), without GWT

but with seismic coefficients, reveals further stability reduction, with Case-II showing the lowest stability (FOS: 1.24 at 30° to 0.90 at 90°), underscoring vulnerability to seismic forces, whereas Cases III and IV, including soil nails, exhibit better stability (Case-IV: 1.56 at 30° to 1.24 at 90°). Scenario (D), encompassing both GWT and seismic coefficients, results in the lowest overall FOS values, particularly in Case-II (FOS: 1.05 at 30° to 0.60 at 90°), but Case-IV demonstrates the highest FOS (1.55 at 30° to 1.23 at 90°), emphasizing the critical role of soil nails under combined adverse conditions.

3.4.1 Correlation matrix observation for different soil slope cases and scenarios

The correlation matrix analysis Fig. 25 revealed several key insights regarding the factors influencing soil slope stability. Strong positive correlations were identified between the use of soil nails and higher FOS values, confirming the significant enhancement of slope stability through soil nails by mitigating the effects of GWT and seismic activity. It was observed that the presence of GWT and seismic coefficients generally correlated with lower FOS values, indicating their destabilising impact on slope stability. The interdependencies among factors such as soil composition, slope angle, GWT, and seismic forces

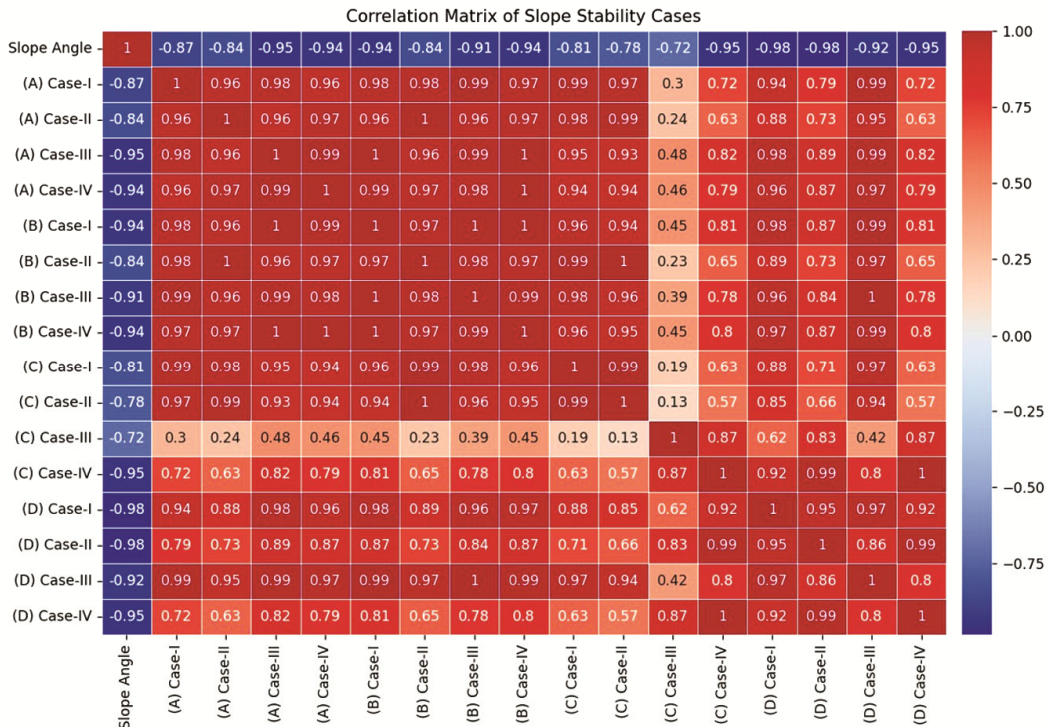


Fig. 25 — Correlation matrix for different soil slope cases and scenarios.

were identified, highlighting the importance of considering these relationships in slope stability analysis and design. Steeper slope angles (Θ) were found to correlate with lower FOS values, emphasising the increased risk of landslides at higher inclinations and underscoring the need for more robust stabilization measures for steeper slopes. Scenarios incorporating both soil nails and measures addressing GWT and seismic impacts showed better stability outcomes compared to those without such measures, suggesting that a combination of stabilisation techniques provides enhanced slope stability under complex conditions. Overall, the correlation matrix analysis in Fig. 25 offered a clear understanding of the key factors affecting soil slope stability, providing valuable insights for designing effective landslide mitigation strategies and ensuring the safety and stability of soil slopes under various environmental conditions.

3.4.2 Comparative Analysis of Slope Stabilisation Studies Across Varied Slope Angles

In this study, to ensure the reliability of the simulation results, various studies based on different parameters were considered for comparison and validation. In this paper, four cases were examined: Case-I (slope without soil nails and surcharge load), Case-II (slope without soil nails but with surcharge load), Case-III (slope with soil nails and surcharge load), and Case-IV (slope with soil nails but without surcharge load). Case-IV consistently exhibited the highest FOS values, indicating superior stability, while Case-I demonstrated the lowest values, suggesting poorer stability conditions compared with Case-IV (refer to Fig. 26). This finding underscores the critical role of soil nails in slope stabilisation.

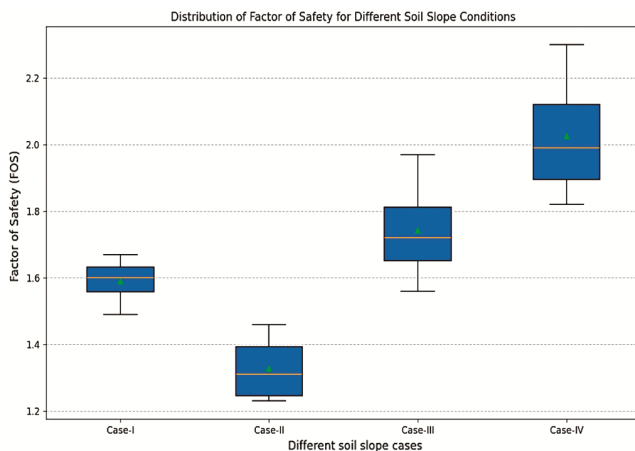


Fig. 26 — Factor of safety (FOS) w.r.t. different soil slope cases.

Additionally, the FOS was observed by considering various soil slope angles from 30° to 90° , revealing that as the slope angle increases, the FOS decreases (refer to Fig. 27).

The comparative analysis of FOS across different studies provides valuable insights into slope stability under varied conditions. In Kaothon *et al.*'s (2021) ⁶¹, the effect of nail spacing on slope stability was investigated across various slope angles (45° , 55° , 65° , and 75°), showing a trend of decreasing FOS with increasing slope angle, with values ranging from 1.75 to 1.5. Chatterjee and Murali Krishna (2019) ⁶¹ studied slope stability under rainfall infiltration, noting higher FOS values for shallower slopes and a decrease with steeper angles (from 26.56° to 65°) across different soil types (refer to Table 3). This decline in FOS aligns with the impact of surcharge loads observed in the present study.

The presence of soil nails without additional surcharge load in the present study aligns with the findings of Chatterjee and Krishna (2019) ⁶², indicating improved stability with soil reinforcement. These observations underscore how environmental

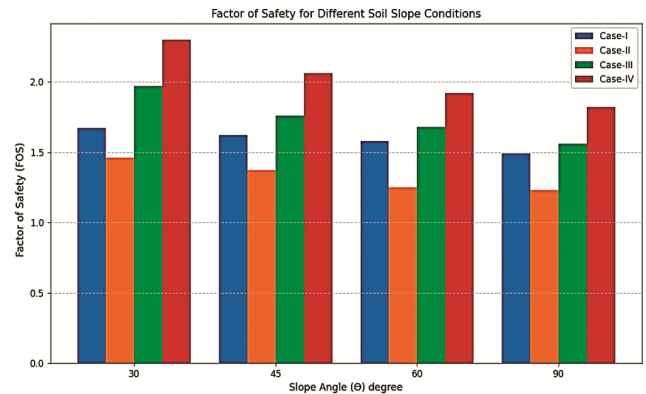


Fig. 27 — Factor of safety (FOS) w.r.t. different soil slope angles (Θ).

Table 3 — Properties of soils used in Chatterjee and Murli Krishna's (2019) study

Property	Soil-1	Soil-2	Soil-3*
Specific gravity	2.61	2.44	2.7
Liquid limit (%)	46	39	41.5
Plastic limit (%)	23	Nonplastic	23.2
USCS classification	CL	SM	CL
c (kN/m3)	17.6	16.8	19
C' (kPa)	10	0	25
ϕ' (0)	30	36	18
ϕ_b (0)	30	36	18
Saturated Permeability, m/s	8.38×10^{-6}	6.6×10^{-5}	8.3×10^{-7}

* Soil-3 properties taken from Kellezi *et al* (2005) ⁶³ study

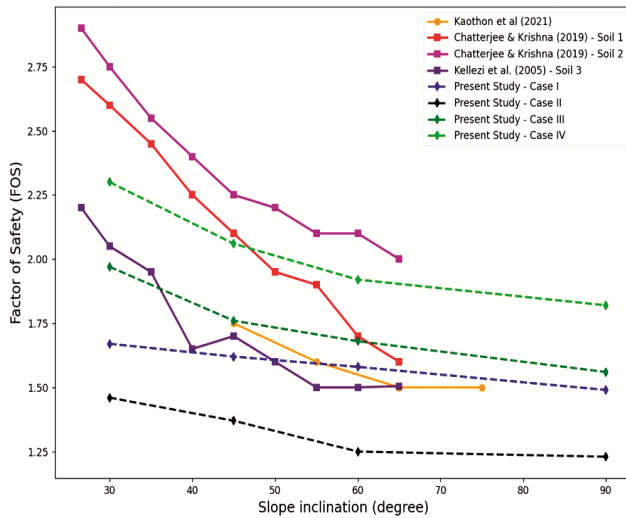


Fig. 28 — Comparison of Slope Inclination vs FOS across various studies.

and loading factors significantly influence slope stability assessments. The present study's findings also align with those of Chatterjee and Krishna (2019)⁶² and Kaothon *et al.* (2021)⁶¹ regarding soil slope inclination, as both observed that with an increase in soil slope angle, the FOS decreases (refer to Fig. 28). These results underscore the importance of considering soil nails and slope angle in slope stability analysis, providing a comprehensive understanding of how these factors interact to influence the FOS.

4. Conclusion

The findings from this study highlight the critical importance of soil nailing as a sustainable and efficient method for enhancing slope stability under various loading and geometric conditions. By conducting an extensive numerical analysis, this study explores the performance of soil nails in mitigating both horizontal (δ_x) and vertical displacements (δ_y) under surcharge (Q) and without surcharge conditions, along with advanced strain-based assessments such as plastic deviatoric strain and plastic volumetric strain distributions. The investigation also evaluated the influence of increasing slope angles (Θ) from 30° to 90° on the Factor of Safety (FOS). These analyses collectively offer a comprehensive understanding of how soil nails perform under realistic conditions, providing both theoretical insights and practical implications for geotechnical engineering design. The conclusions drawn from this study are as follows:

- Soil nails reduced horizontal displacement (X-direction) by approximately 25% without surcharge load.
- Under surcharge load, horizontal displacement was reduced by approximately 28.63% with soil nails.
- Vertical displacement (Z-direction) decreased by about 7.63% without surcharge load when soil nails were used.
- Under surcharge conditions, vertical displacement was observed to have a more significant reduction of approximately 24.60%.
- Resultant displacement was reduced by approximately 6.93% without surcharge and by 32.37% with surcharge when soil nails were applied.
- An increase in slope angle from 30° to 90° showed a trend of reduced FOS, indicating a trade-off between slope angle and stability.
- Soil nails were effective in offsetting the stability loss due to steeper slope angles.
- Numerical analyses (e.g., plastic equivalent deviatoric strain, plastic shear strain, and plastic volumetric strain) confirmed the widespread effectiveness of soil nails across the entire slope domain.
- The study highlights soil nails as a reliable technique to prevent erosion, settlement, and slope failure in both natural and engineered environments.
- The effectiveness of soil nails under surcharge and seismic conditions reinforces their value in landslide- and earthquake-prone regions.

Overall, this study not only quantifies the stabilising effects of soil nails but also underscores their vital role in ensuring slope integrity under challenging geotechnical scenarios. By integrating conventional FOS analysis with advanced strain evaluation techniques, the findings contribute to a deeper understanding of slope failure mechanisms and the mitigation strategies necessary for long-term stability. These insights are especially relevant for regions vulnerable to heavy rainfall, seismic activity, or infrastructure-induced surcharge loading, where slope failure poses serious safety risks.

Acknowledgements

The work presented in this article is encouraged by Delhi Technological University, Civil Engineering Department.

References

- 1 Ortigao J A R & Sayao A S F J, Handbook of Slope Stabilisation, (Springer-Verlag, Berlin Heidelberg), ISBN 978-3-662-07680-4 (eBook), 2004, p. 355.
- 2 Ebrahimi R & Asakereh A, *Int J Basic Sci Appl Res*, 5 (2016) 113.
- 3 Babu G L S, Srinivasa B R & Srinivas A, *Ground Improv*, 6 (2002) 137.
- 4 Seo H J, Lee I M & Lee S W, *KSCE J Civ Eng*, 18 (2014) 488.
- 5 Elahi T E, Islam M A & Islam M S, *Geotechnics*, 2 (2022) 615.
- 6 Lazarte C A, Elias V, Espinoza R D & Sabatini P J, Soil Nail Walls, FHWA (Washington, D.C.), 2003.
- 7 Chavan D, Mondal G & Prashant A, *Soil Dyn Earthq Eng*, 100 (2017) 480.
- 8 Lozada C, Mendoza C & Amortegui J V, *Int J Civ Eng*, 20 (2022) 1115.
- 9 Masi E B, Tofani V, Rossi G, Cuomo S, Wu W, Salciarini D, Caporali E & Catani F, *Catena*, 222 (2023) 106853.
- 10 Jared N S & Noorasyikin M N, *J Eng Technol Adv*, 6 (2021) 17.
- 11 Ghareh S, *Measurement*, 73 (2015) 341.
- 12 Masi E B, Segoni S & Tofani V, *Geosciences*, 11 (2021) 212.
- 13 Ramteke P C & Sahu A K, *Z Dtsch Ges Geowiss*, 174 (2023) 729.
- 14 Pradhan S P, Vishal V & Singh T N, *Nat Hazards*, 94 (2018) 181.
- 15 Zhuang Y, Xing A, Jiang Y, Sun Q, Yan J & Zhang Y, *Eng Geol*, 298 (2022) 106561.
- 16 Donati D, Stead D & Borgatti L, *Geosciences*, 13 (2023) 52.
- 17 Wan Z & Zhu B, *J Civ Environ Eng*, 42 (2020) 10.
- 18 Ferrero C, Berardi R, Calderini C, Cambiaggi L & Vecchiattini R, *Int J Archit Herit*, 17 (2023) 3.
- 19 Paswan A P & Shrivastava A K, *Water (Switzerland)*, 15 (2023) 1862.
- 20 Qin C & Zhou J, *Acta Geotech*, 18 (2023) 3153.
- 21 Sari M J, *Mater Sci*, 19 (2022) 3346.
- 22 Villalobos S A & Villalobos F A, *Transp Geotech*, 26 (2021) 100454.
- 23 Rawat S & Gupta A K, *Electron J Geotech Eng*, 21 (2016) 5577.
- 24 Rashid A S A, Faizi K, Kalatehjari R & Nazir R, *Electron J Geotech Eng*, 18Y (2013) 5881.
- 25 Sharma M, Samanta M & Sarkar S, Landslides: Theory, Practice and Modelling, (Springer Netherlands), ISBN 978-3-319-77377-3, 2018, p. 173.
- 26 Schlosser F & Unterreiner P, *Transp Res Rec*, 1330 (1991) 72.
- 27 Nguyen H B K, Rahman M M & Karim M R, *Front Built Environ*, 9 (2023).
- 28 Rajhans P, Ekbote A G & Bhatt G, *Mater Today Proc*, 65 (2022) 735.
- 29 Filho A L D, Cavalcante E H, Cardoso J C R, Cavalcanti J & D. de A, *Soils Rocks*, 45 (2022).
- 30 Liu S, Su Z, Li M & Shao L, *Eng Geol*, 273 (2020) 105673.
- 31 Ersoy H, Kaya A, Angin Z & Dağ S, *J Earth Syst Sci*, 129 (2020) 82.
- 32 He Y, Wang X Y, Yuan R, Liu K W & Zhuang P Z, *Math Probl Eng*, (2019).
- 33 He Y, Cai Z, Wang F, Guo C, Xiang B, He C & Liu E, *Bull Eng Geol Environ*, 82 (2023) 70.
- 34 Lazorenko G, Kasprzhitskii A, Kukharskii A, Kochur A & Yavna V, *Transp Eng*, 2 (2020) 100028.
- 35 Nasvi M C M & Krishnya S, *Indian Geotech J*, 49 (2019) 620.
- 36 Sazzad M, Atful Hie A B K M & Hossain S, *Int J Adv Struct Geotech Eng*, 5 (2016).
- 37 Su Z & Shao L, *Eng Geol*, 280 (2021) 105910.
- 38 Wang L, Zhang X, Zaniboni F, Oñate E & Tinti S, *Math Geosci*, 53 (2021) 81.
- 39 Ahmad F, Tang X, Hu J, Ahmad M & Gordan B, *Comput Model Eng Sci*, 33 (2023) 455.
- 40 Ahmadi M M & Borghei A, *Scientia Iranica*, 25 (2018) 140.
- 41 Li Z & Xiao S, *Geotech Geol Eng*, 41 (2023) 1893.
- 42 Ng C W W, Crous P A, Zhang M & Shakeel M, *Comput Geotech*, 141 (2022) 104525.
- 43 Pinyol N M, Di Carluccio G & Alonso E E, *Eng Geol*, 297 (2022) 106478.
- 44 Sumartini W O, Hazarika H, Kokusho T & Ishibashi S, *Geotech Eng*, 55 (2021).
- 45 Zhou J & Qin C, *Comput Geotech*, 158 (2023) 105396.
- 46 Ramteke P C & Sahu A K, *Sadhana*, 49 (2024) 62.
- 47 Jain N, Roy P, Martha P R, Jalan P & Nanda A, Landslide Atlas of India, NRSC/ISRO Special Publication, Document No. NRSC-RSA-GSG-GMED-FEB2023-TR-0002167-V1.0, 2023.
- 48 Mohammad Zaki M F, Wan Ahmad W A A, Ayob A & Ying T K, *Appl Mech Mater*, 695 (2014) 526.
- 49 Panah A K & Majidian S, *Geomech Eng*, 5 (2013) 37.
- 50 Chakrabarti B & Shivananda P, *Int J Res Advent Technol*, 7 (2019) 351.
- 51 Zhao J & Shao L T, *Rock Soil Mech (Yantu Lixue)*, 29 (2008).
- 52 Eyyüggiller M M & Ülker M B C, *8th Geotechnical Symposium*, İTÜ Süleyman Demirel Kültür Merkezi, Istanbul, (2019).
- 53 Al-Shayea N A, Mohib K R & Baluch M H, *Int J Damage Mech*, 12 (2003) 305.
- 54 Yang Y, Wu W & Zheng H, *Int J Rock Mech Min Sci*, 164 (2023) 105358.
- 55 Pei H F, Li C, Zhu H H & Wang Y J, *Math Probl Eng*, 2013 (2013).
- 56 Singh V P & Babu G L S, *Geotech Geol Eng*, 28 (2010) 299.
- 57 Ramteke P C & Sahu A K, *Z Dtsch Ges Geowiss*, 3 (2024) 417.
- 58 Solyaev Y & Babaytsev A, *Compos B Eng*, 224 (2021) 109145.
- 59 Seyedan S & Sołowski W T, *Adv Civ Eng*, 2019 (2019).
- 60 Federico A, *Geotechnique*, 39 (1989) 711.
- 61 Kaothon P, Chhun K T & Yune C Y, *Int J Geo-Eng*, 12 (2021) 31.
- 62 Chatterjee D & Murali Krishna A, *Indian Geotech J*, 49 (2019) 708.
- 63 Kellezi L, Allkja S & Hansen P B, *Proc. Int. Assoc. Comput Methods Adv Geomech*, Torino, Italy, 2005.